ISSN 0021-3640, JETP Letters, 2023, Vol. 117, No. 4, pp. 257–261. © The Author(s), 2023. This article is an open access publication.
Russian Text © The Author(s), 2023, published in Pis'ma v Zhurnal Eksperimental'noi i Teoreticheskoi Fiziki, 2023, Vol. 117, No. 4, pp. 254–258.

ASTROPHYSICS AND COSMOLOGY

Muons in EASs with $E_0 = 10^{19}$ eV According to Data of the Yakutsk Array

A. V. Glushkov[a], *, K. G. Lebedev[a], and A. V. Saburov[a]

[a] *Shafer Institute of Cosmophysical Research and Aeronomy, Siberian Branch, Russian Academy of Sciences, Yakutsk, 677891 Russia*

**e-mail: glushkov@ikfia.ysn.ru*

Received September 30, 2022; revised January 8, 2023; accepted January 13, 2023

Lateral distribution functions of particles in extensive air showers with the energy $E_0 \approx 10^{19}$ eV recorded by ground-based and underground scintillation detectors with a threshold of $E_\mu \approx 1.0 \times \sec\theta$ GeV at the Yakutsk array during the continuous observations from 1986 to 2016 have been analyzed using events with zenith angles $\theta \le 60°$. Experimental functions have been compared to the predictions obtained with the QGSJet-01-d hadron interaction model by applying the CORSIKA code. The entire dataset indicates that cosmic rays consist predominantly of protons.

DOI: 10.1134/S002136402360009X

1. INTRODUCTION

In recent years, a problem of muon excess in extensive air showers (EAS) has arisen in several experiments in comparison with model predictions [1]. Many collaborations are involved in solving this problem. Different datasets are compared using the parameter

$$z = \ln(\rho_\mu^{\exp}/\rho_\mu^{p})/\ln(\rho_\mu^{\mathrm{Fe}}/\rho_\mu^{p}), \qquad (1)$$

where $\rho_\mu^{\exp}$ is the muon density measured in the experiment and ρ_μ^{p} ρ_μ^{Fe} are the muon densities calculated for EASs initiated by primary protons and iron nuclei in this experiment, respectively. A combined analysis of the data from eight research groups (EAS-MSU, IceCube Neutrino Observatory, KASCADE-Grande, NEVOD-DECOR, Pierre Auger Observatory, SUGAR, Telescope Array, and Yakutsk) showed that model calculations are in agreement with muon measurements to 10^{16} eV. However, the situation changes with a further increase in the primary energy. A significant spread of the z value is observed, especially in inclined showers [2] and at large distances from the shower axis [3]. Muon densities measured at the Yakutsk array in showers with $E_0 \ge 10^{18}$ eV and $\langle\cos\theta\rangle = 0.9$ at a distance of 300 m from the axis gave the value $z \approx 0$ with the QGSJet-01-d model and negative values with the QGSJet-II-04 and EPOS-LHC models [1]. In [4], the fraction of muons was investigated at distances 300, 600, and 1000 m from the axis in showers with $E_0 \approx 10^{17.7-19.5}$ eV and $\langle\cos\theta\rangle = 0.9$. The agreements with the QGSJet-01-d model was confirmed for primary protons ($z \approx 0$). Here, we continue to study the fraction of muons in EASs with the energy $\approx 10^{19}$ eV in a wide range of zenith angles.

2. LATERAL DISTRIBUTION OF EAS PARTICLES

2.1. Calculation of Mean Lateral Distribution Functions

The responses of ground-based and underground scintillation detectors of the Yakutsk array to EASs initiated by primary particles with the energy above 10^{17} eV were calculated in [5, 6] with a set of artificial showers generated with the CORSIKA code [7] using the QGSJet-01-d [8] and QGSJET-II 04 models [9]. The FLUKA2011 code [10] was chosen to describe hadron interactions at energies below 80 GeV. Showers were simulated with zenith angles 0°–60° in the energy range of 10^{17}–$10^{19.5}$ eV with a logarithmic step of $\Delta\log(E_0) = 0.5$. The calculations involved the thin-sampling mechanism [11] with the thinning level $E_{\mathrm{thin}} = 10^{-6}$–$10^{-5}$ and the weight limit for all components $w_{\max} = E_0 E_{\mathrm{thin}}$. For each set of the input parameters (E_0, θ), from 200 to 500 events were generated. Using these events, mean lateral distribution functions (LDFs) of the detector response were obtained with the radial binning of the distance from the axis with a step of $\Delta\log(R) = 0.04$ step. Figure 1 exemplifies a calculated LDF for the response in ground-based (all) and underground (muons) scintillation detectors of the Yakutsk array in events originated from different primary particles. Figure 2 shows responses from par-

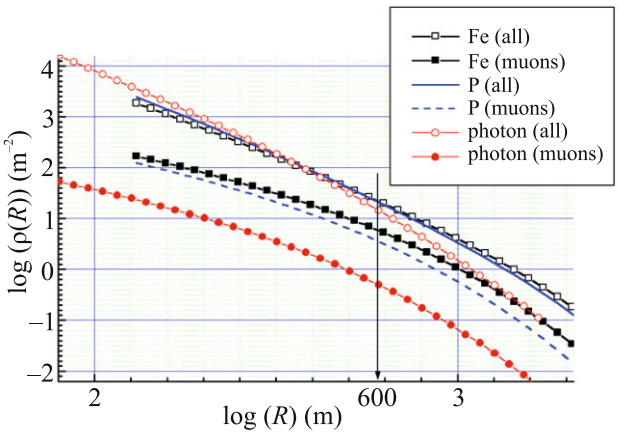

Fig. 1. (Color online) Lateral distribution functions of responses in ground-based and underground scintillation detectors with a threshold of $E_\mu \approx 1.0 \times \sec\theta$ GeV in EASs initiates by primary particles with the energy $E_0 \approx 10^{19}$ eV and $\cos\theta = 0.90$ obtained with the QGSjet-01-d model [6].

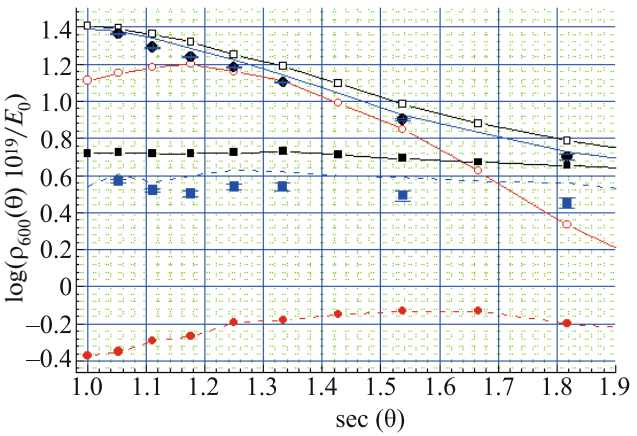

Fig. 2. (Color online) Zenith-angular dependences of responses in ground-based and underground scintillation detectors in showers initiated by primary particles with the energy $E_0 \approx 10^{19}$ eV at a distance 600 m from the axis obtained with the QGSjet-01-d model [6] (notation is the same as in Fig. 1). Dark circles and squares are experimental data (see the main text).

ticles in EASs with $E_0 = 10^{19}$ eV and different zenith angles at a distance of 600 m from the axis. All densities were converted to $E_0 = 10^{19}$ eV by multiplication by normalization factors $10^{19}/\langle E_0\rangle$.

2.2. Event Selection and Processing

The average densities $\langle\rho_s(\theta)\rangle$ and $\langle\rho_\mu(\theta)\rangle$ of all particles and muons in EASs with the threshold energy $E_\mu \approx 1.0\sec\theta$ GeV were considered obtained at a distance of 600 m from the axis in events with mean arrival zenith angles $\langle\cos\theta\rangle = 0.95$, 0.90, 0.85, 0.80, 0.75, 0.65, and 0.55. Experimental LDFs of both components were calculated in zenith-angle intervals $\Delta\cos\theta = 0.1$ with the energy increment $\Delta\log E_0 = 0.2$. We selected showers whose axes were located in a circle with a radius of 1 km around the array center and were determined with an accuracy of no worse than 50 m. The accuracy of evaluation of $\rho_{s,600}(\theta)$ in individual events was above 10%. The primary energy of showers was determined by the formula [12]

$$E_0 = (3.76 \pm 0.3)\times 10^{17}(\rho_{s,600}(0°))^{1.02\pm0.02}\,[\text{eV}], \quad (2)$$

with

$$\rho_{s,600}(0°) = \rho_{s,600}(\theta)\exp((\sec\theta - 1)\times 1020/\lambda)\,[\text{m}^{-2}], \quad (3)$$

where λ is the absorption length shown in Fig. 3 and $\rho_{s,600}(\theta)$ is the density determined in the experiment. The mixed composition was taken from the experiment reported in [12]. Relation (2) unambiguously relates $\rho_{s,600}(0°)$ to E_0 at any cosmic ray composition since LDFs of cascade particles in EASs intersect each other at $R \approx 600$ m. In the case of primary photons, all three LDFs intersect at $R \approx 450$ m (Fig. 1). When calculating LDFs, particle densities in individual events were multiplied by a normalization coefficient $\langle E_0\rangle/E_0$ ($\langle E_0\rangle$ is the average energy in a group) and averaged in distance intervals $[\log(R_i),\ \log(R_i) + 0.04]$. Average particle densities in these intervals were determined as:

$$\langle\rho_s(R_i)\rangle = \left(\sum_{k=1}^{N}\rho_k(R_i)\right)/N, \quad (4)$$

where N is the number of detector readings at a given distance from the axis. The resulting mean LDFs were approximated by the function

$$\rho_s(R,\theta) = \rho_{s,600}(\theta)(600/R)^2(608/(R+8))^{b_s-2} \times ((600 + R_1)/(R + R_1))^{10}, \quad (5)$$

where $R_1 = 10^4$ m and $\rho_{s,600}(\theta)$ and b_s are the free parameters determined by minimizing χ^2.

The muon LDF was constructed in a similar way. Average particle densities were determined as

$$\langle\rho_\mu\rangle(R_i)\rangle = \left(\sum_{n=1}^{n_1}\rho_n(R_i)\right)/(N_1 + N_0), \quad (6)$$

where N_1 and N_0 are the numbers of nonzero and zero readings of muon detectors, respectively, at distances in the intervals $[\log(R_i),\ \log(R_i) + 0.04]$.

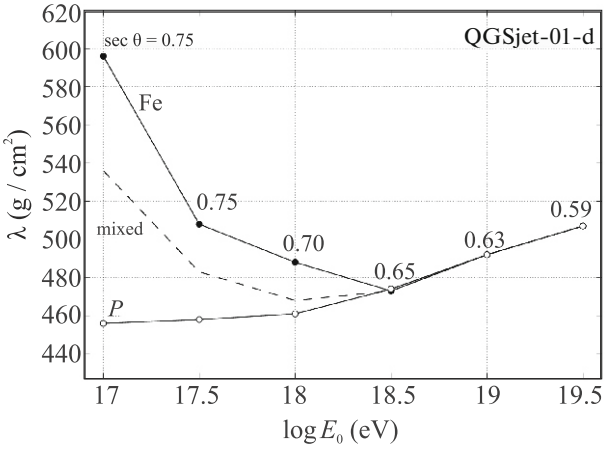

Fig. 3. Energy dependence of the absorption range in Eq. (3) used in the recalculation of $\rho_{s,600}(\theta)$ from inclined to vertical showers according to the QGSjet-01-d model for (*P*) primary protons, (mixed) mixed composition, and (Fe) iron nuclei. Numbers next to the data points indicate limit values of $\cos\theta$ [12].

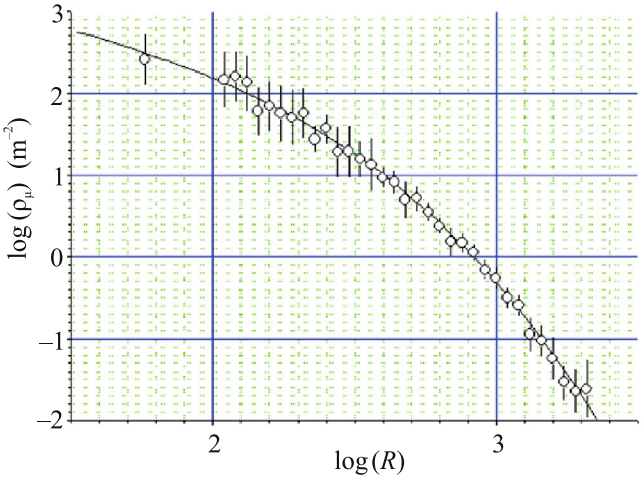

Fig. 4. (Color online) Mean lateral distribution function of muons in showers with $\langle E_0\rangle = 8.93\times10^{18}$ eV and $\langle\cos\theta\rangle \approx 0.8$. The line is approximation (7) with the parameters $\langle b_\mu\rangle = 2.140 \pm 0.027$ and $\langle\log(\rho_{\mu,600})\rangle = 0.488 \pm 0.02$. The processing agreement criterion for all data points is $\chi^2 = 25.1$.

Zero readings N_0 correspond to cases where detectors do not record a single muon while being in the accepting mode. The LDF was approximated by the function

$$\rho_\mu(R,\theta) = \rho_{\mu,600}(\theta)(600/R)^{0.75}(880/(R+280))^{b_\mu-0.75} \times ((600+R_1)/(R+R_1))^{6.5}, \quad (7)$$

where $R_1 = 2000$ m and b_μ and $\rho_{\mu,600}(\theta)$ are the free parameters determined by minimizing χ^2.

3. RESULTS AND DISCUSSION

Figure 4 present one of the mean muon LDFs derived from the experimental data. The density at $R =$ 600 m divided by the average primary energy of EASs equals $\log(\rho_{\mu,600}(37°)\times10^{19}/\langle E_0\rangle) = 0.538 \pm 0.017$. Other experimental data were obtained in a similar manner.

It is seen in Fig. 2 that responses in ground-based and underground detectors from EAS particles are lower than expected responses from primary protons and muon densities are significantly lower than expected values. There are several possible reasons for this result. One of them is the energy estimation in the experiment. The first term in Eq. (2) reflects a systematic error of 8% from the uncertainty of the array calibration method itself [12]. Equation (3) introduces from 0 to 15% due to zenith-angle uncertainty during the transition from $\rho_{s,600}(\theta)$ to the vertical direction. This error is due to dependences of the parameter λ on the primary nucleus atomic number in Eq. (3) (see, e.g., Fig. 2) and on the hadron interaction model. Neither of them are known a priori.

To understand the above result, we assume that shower energy was overestimated by the difference between theory and experiment in the case of ground-based detectors, i.e., by 10%. If the shower energy is reduced by this value, densities measured by ground-based detectors and presented by filled circles in Fig. 2 will be in agreement with the simulated values. Muon densities shown in Fig. 2 will also increase by 10% after energy re-evaluation. The first two sets of the data (at $\sec\theta \approx 1.05$ and 1.11) will agree with the QGSJet-01-d model, whereas the other will remain 10% below the expected values. The results of applying Eq. (1) to the experimental data are summarized in Table 1. The indicated errors include both statistical errors in the calculation of mean LDFs and errors in the reconstruction of individual events (arrival direction, axis coordinates, and energy estimation). It is difficult to distinguish between them and this is not necessary. They are accumulated in the average values $\langle\rho_{s,600}(\theta)\rangle$ and $\langle\rho_{\mu,600}(\theta)\rangle$ (see, e.g., Fig. 3). Values presented in first two columns of Table 1 agree with our estimates given in [1]. The other data are physically meaningless in the z parameter and cannot be explained by methodical distortions of the experiment. We observe another muon puzzle in inclined showers with the

Table 1. Values of z parameter (1) in groups of showers with different zenith angles

$\sec\theta$	1.052	1.111	1.176	1.250	1.333	1.538	1.818
z	0.0	0.0	−0.4	−0.7	−0.7	−0.7	−0.7
$\pm\Delta z$	0.10	0.10	0.2	0.2	0.2	0.3	0.3

Table 2. Fractions of protons and iron nuclei paired with primary photons in the total cosmic ray flux in showers with different zenith angles

secθ	W_p	$\pm\Delta W_p$	W_γ	$\pm Wd_\gamma$	W_{Fe}	$\pm\Delta W_{Fe}$	W_γ	$\pm Wd_\gamma$
1.053	0.98	0.02	0.02	0.02	0.85	0.02	0.15	0.02
1.111	1.00	0.02	0.00	0.02	0.83	0.02	0.17	0.02
1.176	0.95	0.03	0.05	0.03	0.82	0.03	0.18	0.03
1.250	0.92	0.03	0.08	0.03	0.84	0.03	0.16	0.03
1.333	0.91	0.03	0.09	0.03	0.85	0.03	0.15	0.03
1.538	0.91	0.04	0.09	0.04	0.84	0.04	0.16	0.04
1.818	0.87	0.05	0.13	0.05	0.87	0.05	0.13	0.05
average	0.93	0.03	0.07	0.03	0.84	0.03	0.16	0.03

energy $\approx 10^{19}$ eV, but with the opposite sign: a muon deficit is observed in measured densities in comparison with the QGSJet-01-d and QGSJet-II-04 models for primary protons. All above speculations on a hypothetical 10% shift of the energy are conditioned only by the uncertainty in the first term of Eq. (2), which is due to the technique of absolute primary energy calibration at the Yakutsk array [12]. We do not exclude the possibility of its further refinement as the experiment progresses.

At first glance, the reported results are critically sensitive to experimental errors of energy estimation, but this is not entirely the case. If mean LDFs of both EAS components were obtained from the same source dataset with the energy $\langle E_0\rangle$, the fraction of muons $p(600 = \langle\rho_{\mu,600}\rangle/\langle\rho_{s,600}\rangle = (\langle\rho_{\mu,600}\rangle/\langle E_0\rangle)/(\langle\rho_{s,600}\rangle/\langle E_0\rangle)$ in this set hardly depends on the energy. Figure 5 shows the

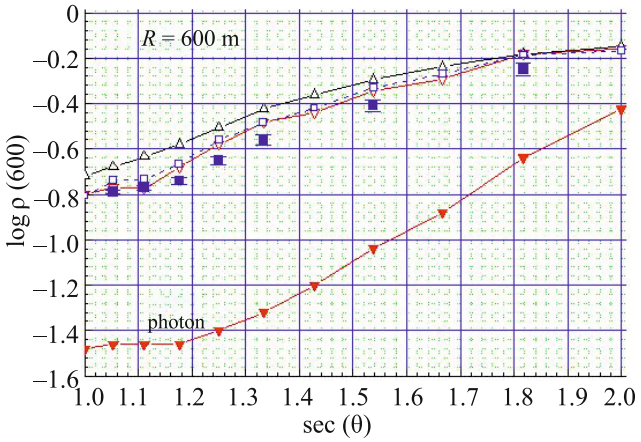

Fig. 5. (Color online) Zenith-angular dependences of the fraction of muons $\langle\log(\rho_{\mu,600}/\rho_{s,600})\rangle$ at a distance 600 m from the axis in the EAS with $E_0 = 10^{19}$ eV initiated by (empty upward triangles) primary protons and (empty downward triangles) iron nuclei according to the QGSjet-01-d model and by (empty squares) primary protons according to the QGSjet-II-04 model [6]. Filled squares are experimental data.

fraction of muons obtained from the data presented in Fig. 2. The deficit of the measured muon component compared to the QGSjet-01-d and QGSjet-II-04 models for primary protons is directly seen. In our opinion, this problem can be solved under the assumption that the total cosmic ray flux contains a certain fraction of primary photons, which yield almost an order of magnitude less muons (see Figs. 2 and 3). There are several estimates of the upper limit of the photon fraction in cosmic rays in this energy region [13–15]. According to the Yakutsk array, it is 10% [13]. Among 33 showers with energies above 2×10^{19} eV considered in [12], there are two events with a low muon content (6%) with zenith angles of 18° and 42°. Our calculations showed that the fractions of primary nuclei and photons in the total cosmic ray flux can be estimated by the formulas

$$W_A = \log(P_{\exp}(\theta)/P_\gamma(\theta))/\log(P_A(\theta)/P_\gamma(\theta)), \quad (8)$$

$$W_\gamma = 1 - W_A, \quad (9)$$

respectively. The results are summarized in Table 2, where only statistical errors following from the analysis of mean LDFs are presented. The first four columns correspond to the proton–photon pair. It is seen that the mean fraction of protons in these groups with $\sec\theta = 1.053$ and 1.111 (first two rows) is 0.99 ± 0.01, which differs from other five rows, where its average value is 0.91 ± 0.03. The results for a hypothetical pair iron–photon are also presented in Table 2. In the latter case, agreement with the experiment can be achieved at the 16% fraction of primary photons in the total cosmic ray flux.

4. CONCLUSIONS

The zenith-angular dependences of particle densities $\langle\rho_\mu(600,\theta)\rangle$ and $\langle\rho_s(600,\theta)\rangle$ from the total event sample with $E_0 \approx 10^{19}$ eV have been analyzed by calculating mean lateral distribution functions of both components (Fig. 2). The results do not exclude that the energy estimated by Eq. (2) should be assumingly reduced by 10%. This assumption requires further

comprehensive analysis. The fraction of muons $\rho_{\mu,600}/\rho_{s,600}$ in showers with zenith angles $\theta \le 38°$ presented in Fig. 5 indicates that the cosmic ray mass composition in this energy region is close to protons. We reported this conclusion in several previous works [4, 16–19], where agreement between experimental data of the Yakutsk array and predictions of the QGSjet-01-d and QGSjet-II-04 models was noted. Some muon deficit is observed in inclined showers. The z parameter (1) in these events is negative and becomes physically meaningless (see Table 1). In our opinion, this difficulty is not due to the experimental error of the primary energy estimate, though this cannot be excluded completely for strongly inclined events. A more detailed analysis is needed for this case. The results obtained can be interpreted under the assumption of the presence of a 6–9% primary photons fraction in the total cosmic ray flux. We are going to continue study in this direction.

CONFLICT OF INTEREST

The authors declare that they have no conflicts of interest.

OPEN ACCESS

REFERENCES

1. H. P. Dembinski, J. C. Arteaga-Velázquez, L. Cazon, et al., EPJ Conf. **210**, 02004 (2019).
2. A. Aab et al. (Pierre Auger Collab.), Phys. Rev. Lett. **117**, 192001 (2016).
3. R. U. Abbasi et al. (Telescope Array Collab.), Phys. Rev. D **98**, 022002 (2018).
4. A. V. Glushkov, K. G. Lebedev, and A. V. Saburov, Bull. Russ. Acad. Sci.: Phys. (2023, in press); arXiv: 2301.12268 [astro-ph.HE] (2023).
5. A. V. Glushkov, M. I. Pravdin, and A. Sabourov, Phys. Rev. D **90**, 012005 (2014).
6. A. V. Saburov, Cand. Sci. (Phys. Math.) Dissertation (Inst. Nucl. Res. RAS, Moscow, 2018).
7. D. Heck, J. Knapp, J. N. Capdevielle, G. Schatz, and T. Thoun, FZKA Report No. 6019 (Forshungszentrum Karlsruhe, 1988).
8. N. N. Kalmykov, S. S. Ostapchenko, and A. I. Pavlov, Nucl. Phys. B Proc. Suppl. **52**, 17 (1997).
9. S. Ostapchenko, Phys. Rev. D **83**, 014018 (2011).
10. A. Ferrari, P. R. Sala, A. Fassó, and J. Ranft, *FLUKA: A Multi-Particle Transport Code* (CERN, Geneva, 2005).
11. W. R. Nelson, H. Hirayama, and D. W. O. Rogers, Report SLAC-R-265 (SLAC, Stanford, 1985).
12. A. V. Glushkov, M. I. Pravdin, and A. V. Saburov, Phys. At. Nucl. **81**, 575 (2018). https://doi.org/10.1134/S0044002718040049
13. A. V. Glushkov, I. T. Makarov, M. I. Pravdin, et al., Phys. Rev. D **82**, 041101 (2009); arXiv: 0907.0374 (2009) [astro-ph.HE].
14. R. U. Abbasi et al. (Telescope Array Collab.), Astropart. Phys. **110**, 8 (2019).
15. A. V. Glushkov, I. T. Makarov, M. I. Pravdin, I. E. Sleptsov, D. S. Gorbunov, G. I. Rubtsov, and S. V. Troitsky, JETP Lett. **87**, 190 (2008).
16. A. V. Glushkov and A. V. Saburov, JETP Lett. **100**, 695 (2014).
17. A. V. Glushkov and A. V. Saburov, J. Exp. Theor. Phys. **119**, 848 (2014).
18. A. V. Glushkov, M. I. Pravdin, and A. V. Saburov, Astron. Lett. **44**, 588 (2018). https://doi.org/10.1134/S106377371810002X
19. A. V. Glushkov and A. V. Saburov, JETP Lett. **109**, 59 (2019).